Paracrine TGF-β Signaling Counterbalances BMP-Mediated Repression in Hair Follicle Stem Cell Activation

Naoki Oshimori[1] and **Elaine Fuchs**[1,*]

[1]Howard Hughes Medical Institute, Laboratory of Mammalian Cell Biology and Development, The Rockefeller University, New York, NY 10065, USA

SUMMARY

Hair follicle (HF) regeneration begins when communication between quiescent epithelial stem cells (SCs) and underlying mesenchymal dermal papillae (DP) generates sufficient activating cues to overcome repressive BMP signals from surrounding niche cells. Here, we uncover a hitherto unrecognized DP transmitter, TGF-β2, which activates Smad2/3 transiently in HFSCs concomitant with entry into tissue regeneration. This signaling is critical: HFSCs that cannot sense TGF-β exhibit significant delays in HF regeneration, whereas exogenous TGF-β2 stimulates HFSCs in vivo and in vitro. By engineering TGF-β- and BMP-reporter mice, we show that TGF-β2 signaling antagonizes BMP signaling in HFSCs but not through competition for limiting Smad4-coactivator. Rather, our microarray, molecular, and genetic studies unveil *Tmeff1* as a direct TGF-β2/Smad2/3 target gene, expressed by activated HFSCs and physiologically relevant in restricting and lowering BMP thresholds in the niche. Connecting BMP activity to an SC's response to TGF-βs may explain why these signaling factors wield such diverse cellular effects.

INTRODUCTION

Tissue homeostasis and regeneration are regulated through balancing quiescence and activation of SCs. HFs offer a unique opportunity to explore this process. Throughout adult life, they undergo dynamic, synchronized cycles of degeneration (catagen), quiescence (telogen), and regeneration (anagen) (Millar, 2002; Schmidt-Ullrich and Paus, 2005; Blanpain and Fuchs, 2009). During telogen, which can last for months, HFSCs are quiescent and reside within a specialized microenvironment called the bulge (Cotsarelis et al., 1990). Within this niche, HFSCs surround the hair shaft produced in the previous cycle. Throughout telogen, the base of the bulge, called the secondary hair germ (HG), directly abuts the underlying DP, a key signaling center for HFSCs.

The telogen→anagen transition relies upon DP-HFSC cross-talk to generate the necessary threshold of activating factors. In addition to Wnt-activating cues (Greco et al., 2009; Enshell-Seijffers et al., 2010; Rabbani et al., 2011), bone morphogenetic protein (BMP) inhibitory factors play a central role in the anagen-promoting process (Kulessa et al., 2000; Botchkarev et al., 2001; Zhang et al., 2006). Upon activation, HFSCs in the HG are the first

*Correspondence: fuchslb@rockefeller.edu.

to proliferate and initiate HF regeneration, whereas HFSCs within the bulge become active several days later (Greco et al., 2009).

As the new HF emerges, the DP stimulus is pushed increasingly further from niche SCs, which return to quiescence (Hsu et al., 2011). By contrast, throughout anagen, relatively undifferentiated bulge cell progeny along the outer root sheath (ORS) accelerate proliferation as they approach the DP. This fuels a steady production of transiently amplifying (TA) matrix cells, which undergo a few divisions while in contact with DP and then terminally differentiate to form the hair and inner root sheath (IRS). At the anagen→catagen transition, matrix cells apoptose and the DP retracts upward along with the dying/differentiating epithelial strand. As the HF reenters telogen, BMPs from the inner layer of non-SC niche cells (Hsu et al., 2011) and from surrounding dermal tissue (Plikus et al., 2008) impose a threshold, which must be overcome to initiate the next cycle.

BMPs belong to a superfamily that includes transforming growth factor βs (TGF-βs). TGF-βs function in tissue morphogenesis, homeostasis, and cancer by regulating diverse biological processes including proliferation, apoptosis, differentiation, and extracellular matrix (ECM) production (Siegel and Massagué, 2003). Skin epithelial cells express distinct Ser/Thr kinase receptors for both BMP and TGF-β pathways. These differentially propagate their respective signals by phosphorylating Smad1/5/8 (BMP) or Smad2/3 (TGF-β), which form distinct bipartite transcription factors with Smad4 (ten Dijke and Arthur, 2007). Although BMP's inhibitory effects are well documented, the effects of TGF-β signaling on HFSCs remains largely unexplored.

TGF-βs potently inhibit proliferation of interfollicular epidermis (IFE), and postnatal loss of TGF-β signaling renders skin prone to tumorigenesis (Bierie and Moses, 2006; Guasch et al., 2007; Massagué, 2008). Conditional loss of TGF-β receptor II (*TβRII*-cKO) results in loss of canonical TGF-β signaling in the skin epithelium, but overall tissue morphology remains intact (Guasch et al., 2007). Intriguingly, full gene knockout studies of the receptor ligands show three different effects on embryonic HF development: delay (*TGFβ2*), enhancement (*TGFβ1*), or none (*TGFβ3*) (Foitzik et al., 1999). Given these complexities, we turned to the following key questions. Do TGF-βs play a role in adult HF regeneration and if so, how? Which TGF-β(s) are involved, which cells transmit the signals, and what cells are affected? How might TGF-β signaling within the niche influence the balance between HFSC quiescence and activation, and by what mechanism? Here we address these points and in so doing, shed important new light on the signaling crosstalk within the SC niche.

RESULTS

TGF-β Signaling Is Transiently Activated in Stem Cells during the Telogen→Anagen Transition

To determine whether and how TGF-βs might affect HF regeneration, we first verified the specificity of our anti-phospho-Smad2 antibodies. Upon TGF-β exposure in vitro, primary wild-type (WT) mouse epidermal keratinocytes (1°MKs) exhibit phosphorylation and nuclear translocation of Smad2, which can be detected by immunoblotting of nuclear extracts and immunofluorescence. This band and nuclear staining were absent in the equivalent 1°MKs from *Tgfbr2*^{fl/fl};*Tg(KRT14-Cre)1Efu* (*TβRII*-cKO) mice whose skin epithelium lacks TβRII, an essential component of the TGF-β receptor (Figures S1A and S1B available online; Guasch et al., 2007). Using WT and *TβRII*-cKO mice, we then turned to in vivo analyses.

During normal homeostasis, epidermis displayed little or no signs of active TGF-β signaling (not shown). Postnatally, the first signs of TGF-β signaling appeared in telogen, when pSmad2^{+} nuclei were detected in HG cells adjacent to the DP (Figure 1A). As follicles began cycling, nuclear pSmad2^{+} cells also appeared in CD34^{+} HFSCs at the bulge base. By the time full anagen was reached, pSmad2 immunofluorescence was no longer detected in HFSCs (Figure S1C).

The second telogen (marked by two rather than one club hairs) lasted about 4 weeks in control mice. During early and mid-telogen phases, TGF-β activity was weak. As telogen ended, pSmad2 reappeared in the P-cadherin[+] HG and lower bulge (Figure 1B). Notably, pSmad2 was detected ~5 days before this proliferative activity was seen within the HG (Figure 1C). Similar to the first hair cycle, most HG cells in early anagen exhibited TGF-β signaling, but as the expanding HG engulfed the DP and formed the matrix, pSmad2 waned.

To further examine TGF-β signaling, we engineered a lentivirus harboring a canonical TGF-β-reporter driven by Smad2/3-Smad4 binding sites (Figure 1D). In vitro, reporter expression (NLS-mRFP[+]) was detected only in TGF-β-stimulated, transduced (H2B-CFP[+]) 1°MKs from WT and not in *TβRII*-cKO mice (Figure 1E; shown are data for TGF-β2). When transduced by in utero infection into embryonic skin epithelium (Beronja et al., 2010) and then monitored in adult mice, the TGF-β-reporter was active selectively in the WT HG, beginning at late telogen and continuing into early anagen (Figure 1F). Underscoring reporter specificity, similarly transduced *TβRII*-cKO animals showed no signs of reporter activity. These data revealed that nuclear pSmad2 at the telogen→anagen transition is accompanied by pSmad2-mediated active transcription in the HG.

Stem Cell Activation in Hair Follicles Is Delayed when TGF-β Signaling Is Lost

The TGF-β/pSmad2 signaling pattern upon anagen onset paralleled the two-step activation of HFSCs described previously (Greco et al., 2009). To determine whether TGF-β signaling functions in HFSC activation, we analyzed this process in *TβRII*-cKO mice. By 22 days, control HFs had already entered the first anagen and showed proliferating (Ki67^{+}) HG cells, while *TβRII*-cKO HFs were still in telogen (Figure 2A). Because the first WT telogen lasts only 1–2 days, the phenotypic consequences of losing TGF-β signaling to SC activation and tissue regeneration were best visualized by waiting until HFs had entered the extended second telogen. At this time, we clipped hair coats of sex-matched littermates and then followed the emergence of new hairs as the next cycle began (Figure 2B).

In the second telogen, hair growth was so delayed in *TβRII*-cKO mice that 75% coat recovery occurred ~1 month later than normal (Figure 2C). Despite this delay, the final lengths of the four hair types were normal (Figure 2D), as were HF morphologies and established markers (Figure 2E). Thus, once TβRII-deficient SCs were eventually activated, they executed what appeared to be an otherwise normal hair cycle.

The Dermal Papillae Produce a Paracrine TGF-β2 Signal to Activate Canonical TGF-β-Mediated Transcription in Hair Follicle Stem Cells

Because pSmad2^{+} cells appeared at the interface between HG and DP, and after the extended crosstalk period that is required for HFSC activation, we sought to identify the TGF-β ligands involved and the cell population expressing them. A survey of existing microarray data indicated that in adult skin, *TGFβ2* mRNAs might be enriched in DP relative to HG or HFSCs (Greco et al., 2009). Support for this came from real-time quantitative polymerase chain reaction (RT-qPCR) of mRNAs isolated from purified cell populations of late-telogen phase, *Lef1-RFP* transgenic skins. *TGFβ2* mRNAs selectively

were enriched in DP relative to other IFE and HF populations, whereas *TGFβ1* and *TGFβ3* mRNA expression was low and showed no specific enrichment (Figures 3A and S2A).

Immunofluorescence analyses were consistent with these findings. Of the three TGF-βs, only TGF-β2 protein appeared in HFs toward the end of telogen (Figures 3B and S2B). Intercellular TGF-β2 first accumulated at the ECM interface between DP and HG, but by anagen onset, it intensified in the DP, with weaker staining in HGs. Although latent TGF-β complexes can reside within ECM (ten Dijke and Arthur, 2007), TGF-β2 signal intensity in the DP coincided with nuclear pSmad2 in the HG.

To test whether TGF-β2 signaling can precociously activate resting HFSCs, we coinjected recombinant, active TGF-β2 with fluorescent beads into mid-telogen skin dermis, i.e., well before the normal appearance of endogenous TGF-β2 in DP (see experimental design in Figure 3B). In *TβRII*-heterozygous (WT) mice, TGF-β2 injections resulted in Smad2 phosphorylation not only in the HG, but also in IFE and some dermal cells (Figure S2C). By contrast, *TβRII*-cKO skin epithelium was refractory to TGF-β2- mediated Smad2 activation, while dermal cells responded. This result indicated that the effects of DP-derived TGF-β2 on precocious pSmad2 induction rely upon the HG's ability to respond through the canonical receptors. With our TGF-β-reporter mice, we further demonstrated that the signaling involves canonical pSmad2-mediated transcriptional activation (Figure S2D).

TGF-β2 Induces Proliferation in Quiescent Hair Follicle Stem Cells and Propels Them into a Tissue-Regenerating Mode

Bromodeoxyuridine (BrdU) administration and S-phase cell quantification revealed that HGs of WT HFs reacted to TGF-β2 by displaying both nuclear pSmad2 and proliferation (Figures 3C and S2C). Although this further substantiated the sequential order of events we had observed in the normal hair cycle (see Figure 1C), it contrasted with TGF-β's established negative growth effects on epidermal cells, which was also reflected in decreased BrdU incorporation within IFE (Figure 3C). These results indicate that IFE and HF progenitors interpret TGF-β2 differently and further underscore the specificity of the proliferative response of HFSCs to TGF-β2.

TGF-β2's stimulatory effects depended upon close proximity of HFs to the bead injection site and were followed by a precocious hair cycle (Figures 3D, 3E, S2E, and S2F). This differed from similar injections with FGF7, another DP-derived factor that stimulated HG proliferation, but did not kindle a new hair cycle (Greco et al., 2009). Taken together, our findings indicate that in normal homeostasis, DP utilizes TGF-β2 in short-range signaling to stimulate HFSCs at the bulge base. The outcome is canonical TGF-β receptor/pSmad2 transcription that in some way enables them to achieve the activating threshold necessary to flip the telogen→anagen transition switch.

BMP Signaling Is Prolonged when Hair Follicle Stem Cells Cannot Respond to TGF-β2

Throughout the resting phase, high BMP signaling maintains HFSCs in a quiescent state and must be overcome to promote new tissue growth (Andl et al., 2004; Blanpain et al., 2004; Kobielak et al., 2007; Plikus et al., 2008; Rendl et al., 2008; Greco et al., 2009; Hsu et al., 2011). The appearance of TGF-β2 protein in the DP toward the end of telogen coincided with the timing of enhanced mRNAs encoding DP-derived BMP inhibitory factors, including *Sostdc1* and *Bambi* (Greco et al., 2009). Given the seemingly opposing effects of TGF-β2 and BMPs on HFSC quiescence, we wondered whether TGF-β2 might be impacting the BMP pathway, and if so how.

To address this possibility, we first evaluated the consequences of loss of TGF-β signaling on BMP receptor signaling in HFSCs (Figure 4A). In WT HFSCs, nuclear anti-phospho-

Smad1/5/8 immunostaining, a sign of active BMP signaling, was observed throughout early and mid-telogen, but waned toward the end of telogen, coincident with the appearance of pSmad2 (Figure 4A; see also Figure 1B). However, in *TβRII*-cKO HFSCs, pSmad1/5/8 remained high throughout this time (Figure 4A), consistent with the notion that TGF-β signaling negatively affects BMP signaling.

To further explore TGF-β2's effects, we cultured epidermal 1°MKs, where the antiproliferative effects of TGF-βs are well established (Siegel and Massagué, 2003). Indeed, all three TGF-βs promoted comparable Smad2 phosphorylation and induced growth arrest in a monophasic, dose-dependent fashion (Figures S3A–S3E). Consistent with its lower binding affinity to TβRII (Cheifetz et al., 1987; Massagué et al., 1992), ~10× more TGF-β2 (10 versus 1 pM) was necessary to achieve growth inhibition (Figure S3E). Recombinant TGF-βs had no effects on *TβRII*-cKO 1°MKs, thereby confirming the specificity of the response.

Next, we tested cultured HFSCs, purified by fluorescence-activated cell sorting (FACS) of mid-telogen HFs (Figure 4B). At higher concentrations (50–100 pM), TGF-βs reduced both number and size of HFSC colonies. However, at lower concentrations (~10 pM) where epidermal 1°MKs were still growth restricted, HFSC colonies grew larger. This effect was highly reproducible and not seen in *TβRII*-null HFSCs (Figure 4C). In good agreement with our in vivo observations, these results further unveiled the dose dependency of TGF-β's stimulatory effects on HFSCs.

Consistent with HFSC quiescence in and out of the niche in vivo, nuclear pSmad1/5/8 staining was also greater in nascent colonies of HFSCs than in 1°MKs (Figure S3F). This was true for both WT and *TβRII*-null cells, but not *Bmpr1a-cKO* cells, which showed no signs of BMP signaling. Moreover, pSmad1/5/8 staining in WT HFSCs was reduced by exposure to TGF-β2 (Figure S3G).

Further substantiating the antagonistic effects of TGF-β2 on the BMP pathway, we found that BMP4's effects were monophasic and could be partially relieved by TGF-β2 in a TβRII-dependent manner (Figures 4B and 4C). Importantly, neither BMP4 nor TGF-β2 affected the colony size in *Bmpr1a*-cKO HFSCs (Figure 4D). Moreover, even though TGF-β2 on its own no longer exerted effects on colony size as HFSCs were passaged, TGF-β2 still counteracted the negative effects of BMPs that were added exogenously to HFSC cultures (Figure S3H). Thus, the stimulatory growth effects of TGF-βs appeared to be restricted to cells exhibiting active BMP signaling.

To further pursue the notion that TGF-β2 acts positively to overcome BMP inhibitory thresholds and activate HFSCs, we compared TGF-β2's effects to Noggin, an established and potent BMP antagonist (Botchkarev et al., 2001; Plikus et al., 2008). In early telogen, neither Noggin nor TGF-β2 were sufficient to overpower the exceedingly high BMPs within the HFSC niche and dermis. However, in mid-telogen, both Noggin and TGF-β2 precociously diminished nuclear pSmad1/5/8 and induced HG proliferation (Figures 4E and 4F). As endogenous TGF-β2 signaling and BMP signaling blockers rose and dermal BMP waves waned at telogen's end, these effects were less pronounced. Notably, although probably not physiologically relevant, TGF-β1 and TGF-β3 behaved similarly, indicating that it is TGF-β availability and not TGF-β2 per se that is important in the process (Figure 4G).

In contrast to Noggin, TGF-β2's effects were seen only in WT and not *TβRII*-cKO mice. This result was important as it demonstrated that the opposing effects of TGF-β2 on BMP signaling are mediated directly through the TGF-β receptor pathway rather than cross-counter effects on their respective receptors. Moreover, these data provided compelling

complementary evidence that the atypically long telogen of *TβRII*-cKO mice arises from protracted BMP signaling in HFSCs.

Evidence Favoring a TGF-β Target Gene in Hair Follicle Stem Cell Activation

To further probe the antagonistic interaction between TGF-β2 and BMP signaling, we engineered and tested a BMP-reporter lentivirus (Figure 5A). In vitro, transduced WT and *TβRII*-null, but not *Bmpr1a*-null, 1°MKs displayed BMP-reporter activity in response to BMP4. In vivo, WT HFSCs showed concomitant downregulation of both BMP-reporter activity and pSmad1/5/8 at telogen's end. By contrast, *TβRII*-cKO HFSCs sustained BMP-reporter activity and pSmad1/5/8 during this time.

Importantly, our BMP-reporter was specific, and in the absence of BMPs, TGF-β2 had little or no effect on its expression (Figure 5B). In contrast, BMP4 strongly stimulated BMP-reporter (ZsGreen) expression. TGF-β2 dampened this activity specifically in WT and not in *TβRII*-cKO 1°MKs. Moreover, similar results were obtained with cultured, FACS-purified HFSCs. However, HFSCs displayed active BMP signaling in vitro, and hence TGF-β2 alone was sufficient to reduce BMP-reporter activity in HFSCs (Figure 5C). Based upon these results, TGF-β2 appeared to counteract not only extrinsic but also intrinsic BMP signaling.

The dampening effects on BMP signaling were paralleled at the mRNA level and appeared relatively late (12–24 hr) after TGF-β2 treatment (Figure 5D). With 1°MK, this effect was even more obvious when they were pretreated with TGF-β2 prior to adding BMP4 (Figure 5E). Because the reporter differs from control vector only by multimerized Smad1/5/8 binding sites, these results further bolstered the notion that TGF-β2 was specifically affecting canonical BMP signaling at the transcriptional level.

One way of achieving these effects might be through competition between pSmad2/3 and pSmad1/5/8 for a limiting amount of the Smad4 cofactor. Such mechanisms should be refractory to drugs such as cycloheximide, which effectively blocks protein synthesis within minutes in epidermal keratinocytes (Rice and Green, 1979). However, 10–100 μg/ml cycloheximide nearly abrogated the inhibitory effects of TGF-β2 on BMP-reporter expression (Figure 5F; shown are data for 10 μg/ml). Thus, TGF-β2's antagonistic effects appeared to require new protein synthesis.

Further evidence against a Smad4 competition mechanism came from testing whether simultaneous activation of Smad2/3 interfered with the availability of transcriptional cofactor Smad4 for Smad1/5/8. Immunoblot analysis of nuclear and cytoplasmic lysates from TGF-β2, BMP, and TGF-β2/BMP-costimulated (short-term) cells showed that BMP4 stimulated phosphorylation and nuclear accumulation of Smad1/5/8 and that this did not change upon TGF-β2 costimulation (Figure 5G). Conversely, TGF-β2-enhanced phosphorylation and nuclear accumulation of Smad2/3 did not change with BMP4 costimulation. Notably, although nuclear:cytoplasmic ratios of Smad4 increased upon BMP4/TGF-β2 costimulation, there appeared to be ample Smad4 to accommodate both pathways. This was further demonstrated by coimmunoprecipitating Smad4 with Smad1 antibodies. As shown in Figure 5H, complex levels were not diminished by BMP4/TGF-β2 costimulation.

A Search for Relevant TGF-β Target Genes Yields *Tmeff1*, Encoding an Antagonist of the BMP Pathway

In searching for an alternative transcriptional mechanism that could explain TGF-β2's antagonistic effects on BMP signaling, we wondered whether one of pSmad2/3-Smad4's target genes might encode a negative regulator of BMP signaling. To test this hypothesis, we

purified and transcriptionally profiled HFSC mRNAs at times prior to and during peak TGF-β2 expression in the DP.

Microarray profiling and comparative analyses were performed on duplicate sets of HG (YFP$^+$Pcad^{hi}), bulge HFSCs (YFP$^+$ CD34$^+$), and total (YFP$^+$) cells FACS-purified from two pairs of late-telogen/early-anagen female *TβRII*-Het (WT) and cKO littermates (Figures S4A and S4B). As expected, the HG displayed more changes over these times than the other cell populations. Concomitant with TGF-β2 expression, 341 probes (292 genes) were specifically elevated by 2× in the WT HG relative to the bulge or total YFP$^+$ cells. Shown in Table S1, this "activated HG signature" differed from prior HG array data (Greco et al., 2009) in that it was rich in, e.g., cell cycle genes associated with stem cell activation.

In comparing "preactivated" *TβRII*-null and WT HGs, only 40 of these genes were downregulated in *TβRII*-null HGs. By contrast, in comparing their "activated" states, 252 genes were downregulated by 2× in the *TβRII*-null HG (Table S2), and 239 of these were among the "activated HG signature." Although some changes could be more closely linked to HG activation and not specifically to the absence of TGF-β2 signaling, 63 of these genes have evolutionarily conserved Smad2/3-Smad4 sequence motifs within the body of the gene or 5,000 bp 5′ upstream (ECR browser [Ovcharenko et al., 2004]) (Table S3).

Several interesting findings emerged from these comparisons (Figures 6A, S4C, and S5D). *TβRII* ablation did not affect the master transcription factors required for HFSC/HG maintenance. This was true even for Nfatc1, which is known to play a role in HFSC quiescence downstream of BMP signaling (Horsley et al., 2008). Rather, genes relating to (1) BMP inhibition, (2) cell cycle stimulation, and (3) HF lineage-associated transcription were featured among the genes downregulated in late-telogen/early-anagen *TβRII*-cKO versus WT HG. Notably and in contrast to cell cycle genes, inhibitors of BMP signaling remained on the shortlist of putative TGF-β target genes: *Bambi* (4.5×), *Bmper* (3.7×), and *Tmeff1* (6.7×).

After validating the microarray data by RT-qPCR, we examined temporal expression of BMP inhibitor genes after TGF-β2 stimulation in vitro (Figures 6B and 6C). *Bambi* has been reported as a direct target of TGF-β-Smad signaling (Sekiya et al., 2004) and has previously been identified as a possible participant in DP-HG crosstalk (Greco et al., 2009). However, of the three, *Tmeff1* mRNA was not only the sixth most changed putative TGF-β target gene in the *TβRII*-cKO HG signature, but it also displayed more pronounced and sustained induction upon TGF-β2 treatment (Figure 6C). Therefore, we focused on this hitherto unexplored gene in skin for our remaining studies.

To test whether *Tmeff1*'s putative Smad2/3 binding site is indeed utilized, we conducted chromatin immunoprecipitation (ChIP) with Smad2/3 antibodies. Notably, Smad2/3 binding was enriched on the 5′ UTR of the *Tmeff1* gene of WT but not *TβRII*-null 1°MK (Figure 6D). Moreover, this enrichment was observed only when WT cells were stimulated with TGF-β2.

Further evidence linking *Tmeff1* to TGF-β2 signaling came from protein analyses, where Tmeff1 protein displayed kinetics that paralleled *Tmeff1* gene induction in vitro (Figure 6E). In vivo, Tmeff1 protein appeared concomitantly with pSmad2$^+$ cells in (1) HGs activated during normal homeostasis and (2) HGs precociously activated upon intradermal TGF-β injections (Figures 6F, 6G, and S4E). Finally, when *TβRII*-cKO HFSCs eventually initiated their next hair cycle, the activated HGs showed no signs of either Tmeff1 or pSmad2 (Figures 6H, S4F, and S4G). These findings link Tmeff1 directly to TGF-β2 signaling and not merely SC activation.

Functional Evidence that *Tmeff1* Lowers the BMP Threshold for Stem Cell Activation

To investigate whether Tmeff1 is functionally relevant to the TGF-β2-mediated downregulation of BMP signaling, we performed lentiviral *Tmeff1*-shRNA-mediated gene knockdown experiments in BMP-reporter-transduced 1°MK. 1°MK were exposed to BMP4/ TGF-β2 as before, so that control cells would maintain TGF-β2 signaling-dependent suppression of BMP-reporter activity. In striking contrast to scrambled-shRNA where BMP-reporter (ZsGreen) remained silent, cells transduced with *Tmeff1*-shRNA were green (Figure 7A). By contrast, albeit somewhat less effective at knocking down their targets, *Bambi* and *Bmper*-shRNA were considerably less potent at rescuing BMP-reporter activity (Figures S5A and S5B).

In BMP4/TGF-β2-treated cells transduced with *Tmeff1*-shRNA, endogenous *Tmeff1* expression was kept low, and BMP-reporter activity remained elevated. In contrast, *Tmeff1* levels did not affect TGF-β-reporter activity or Smad2 phosphorylation (Figures S5C and S5E). Moreover, *Tmeff1* appeared to be a key mediator of the specific antagonistic effects of TGF-β2 on BMP-reporter activity, because introducing mCherry- or FLAG-tagged Tmeff1 into BMP4-stimulated cells resulted in strong suppression of both Smad1/5/8 phosphorylation and BMP-reporter activity (Figures 7B, S5D, and S5F).

To assess the physiological relevance of Tmeff1, we employed our powerful in utero lentiviral delivery system, which enables stable, efficient, and selective shRNA-knockdown in skin epithelium (Beronja et al., 2010). We transduced mice with two different *Tmeff1*-shRNAs and a scrambled control shRNA. Both *Tmeff1*-shRNAs behaved similarly, ruling out off-target effects. For the purposes here, we show representative skin sections from mice transduced with the most effective *Tmeff1*-shRNA.

At P21, when HFs were in their short first-telogen, Tmeff1 protein was detected only in HGs of scrambled-shRNA- and not in HGs of *Tmeff1*-shRNA-transduced mice (Figure 7C). When adult mice were shaved at the start of their first postnatal anagen (P23–P24), scrambled-shRNA-transduced hair coats regrew with kinetics similar to uninfected littermates, whereas *Tmeff1*-shRNA-transduced animals exhibited a significant delay in hair regrowth (Figures 7D and 7E). By P43, when scrambled-shRNA-transduced HFs had already entered into their second-telogen (two hairs/HF), *Tmeff1*-shRNA-transduced HFs were still in the midst of their first anagen (Figure 7F). Although the extent of these differences varied somewhat with individual infections, the trend was consistent, underscoring *Tmeff1* as a downstream target of TGF-β signaling and important mediator of SC activation at the telogen→anagen transition.

DISCUSSION

TGF-β2: A Player in the Positive Mesenchymal-Epithelial Crosstalk that Leads to Stem Cell Activation

TGF-β2 was previously shown to be positively involved in HF development during embryogenesis (Foitzik et al., 1999; Jamora et al., 2005). Our studies not only extend this to the postnatal hair cycle but further bolster the view set forth by Foitzik et al. (1999) that the responsiveness to TGF-β2 might be different between HFSCs and IFE keratinocytes. Even under the same culture conditions where TGF-β2 showed a positive effect on HFSCs, IFE 1°MKs were still growth restricted, suggesting that intrinsic features underlie these differences. Our results now show that extrinsic and intrinsic BMP signaling is higher in HFSCs than IFEs, constituting a physiological root of their strikingly different responses to TGF-βs.

At the start of telogen, intradermal BMP levels are high but then gradually decline (Plikus et al., 2008). Conversely, BMP inhibitors produced by the DP rise over telogen, thereby reducing the threshold that maintains SC quiescence. Our findings now show that TGF-β2 features prominently in dampening BMP signaling and facilitating HFSC activation. Because *TβRII*-cKO mice eventually enter into the next hair cycle after an unusually prolonged telogen phase, we are able to draw two additional important conclusions: first, that TGF-β2's function is specific to the SC activation step; and second, that SC activation is not governed by a single factor or cell type but rather is exquisitely sensitive and responsive to the comprehensive environment of the HFSC niche.

The HFSC niche is also the residence for melanocyte stem cells (MSCs), which depend upon TGF-β signaling for their maintenance (Nishimura et al., 2010; Tanimura et al., 2011). TGF-β1/2 are present in the IRS cells that appear in early anagen (Tanimura et al., 2011), and we confirmed that pSmad2 is expressed in mature IRS (Figure S1C). However, our findings now add two intriguing new facets to this equation: first, TGF-β2 signaling acts in a short-range and concentration-dependent fashion, as judged by our bead injection and in vitro experiments; and second, DP is the major source of TGF-β2, expressed specifically and transiently at the quiescence→activation transition. Given that DP abuts both HG and MSCs at a stage when they both become activated, it will be interesting in the future to see how this dynamic interplay unfolds. Additionally, while our studies have concentrated on our discovery that TGF-β2 signaling negatively influences BMP signaling in the HFSCs, other signaling pathways, e.g., Wnts and Shh, could be impacted either directly or indirectly, and this could contribute to the TGF-β-related cell-type differences that we and others have observed in the skin.

Antagonistic Crosstalk between TGF-β2 and BMP Signaling and a Role for the Direct TGF-β Target Gene *Tmeff1*

BMP signaling negatively regulates SC proliferation in many niches including the bulge (Zhang et al., 2006; Kobielak et al., 2007; Plikus et al., 2008) and intestinal crypt (Haramis et al., 2004). In both of these cases, BMP signaling appears to suppress Wnt signaling. Although there are multiple means of antagonizing Wnt signaling through BMP signaling (He et al., 2004; Jian et al., 2006; Liu et al., 2006; Zhang et al., 2006; Kobielak et al., 2007), restricting BMP signaling appears to be a key step in promoting SC activation for tissue regeneration. Our discovery of a novel paracrine role for TGF-β2 in dampening BMP signaling unearths a newfound and early importance for TGF-βs at this critical crossroad in SC biology.

We were prompted to delve deeper into the underlying mechanisms when we realized that TGF-β2's communication circuit is launched just prior to anagen onset when HFSCs undergo activation and proliferaton. We initially speculated that competition between pSmad1/5/8 and pSmad2/3 for limiting Smad4 might underlie the antagonistic effects we observed. As negative support for this hypothesis mounted, we turned to an alternative hypothesis, namely that a direct Smad2/3 target gene(s) might encode an inhibitor of BMP signaling.

Consistent with the tight link between TGF-β2 signaling and SC activation, our microarray and comparative analyses of late-telogen/early-anagen *TβRII*-cKO versus Het HGs strongly overlapped with our activated HG signature. Even though many of the shared differentially expressed genes possessed Smad2/3-Smad4 binding motifs, the list was not particularly enriched for such genes, suggesting that only a few may be relevant to TGF-β2's antagonistic effects on BMP signaling. In this regard, *Tmeff1* (also known as *tomoregulin-1*) surfaced and stayed at the forefront.

Tmeff1 is a transmembrane protein containing two follistatin domains and an epidermal growth factor-like domain in its extracellular region. Although comparatively little is known about this protein, several tantalizing reports relate to our findings: first, Tmeff1 blocks BMP2-mediated mesoderm induction in the *Xenopus* embryo, and second, it inhibits signaling of another TGF-β superfamily member, Nodal, through direct binding to the Nodal coreceptor Cripto (Chang et al., 2003; Harms and Chang, 2003). Finally, although the epithelial-mesenchymal transition gene *Snail*, important in embryonic HF morphogenesis (Jamora et al., 2005), did not surface as a relevant TGF-β2 target in the adult HFSC niche, it is intriguing that like *Snail* family members, *Tmeff1* is commonly upregulated during epithelial-mesenchymal transitions (Moreno-Bueno et al., 2006).

Our studies now demonstrate that *Tmeff1* is a direct target of TGF-β signaling. They also uncover a hitherto unrecognized link between TGF-β signaling and the opposing effects of Tmeff1 on BMP signaling at least at Smad1/5/8 phosphorylation events. Given the widespread importance of BMP signaling in controlling adult SC quiescence and the need to restrict it upon SC activation, it will be interesting in the future to explore the extent to which the mechanisms we have uncovered here might represent a common theme in SC biology.

In closing, increasing numbers of reports have surfaced over recent years describing both synergistic and antagonistic effects between TGF-β and BMP signaling pathways (Wang and Hirschberg, 2003; Yew et al., 2005; Izumi et al., 2006; Giacomini et al., 2009; Wrighton et al., 2009; Keller et al., 2011). Indeed, these two cognate pathways seem to be intertwined frequently, although the outputs from their crosstalk are unpredictable. Our findings now provide a functionally important example of this interplay in SC biology and epithelial-mesenchymal crosstalk. In sifting through the possible mechanisms and dissecting physiologically relevant players, the pathway guided us to an interesting example of a target gene induced selectively by one of these signaling pathways that can potently impact the other signaling pathway.

EXPERIMENTAL PROCEDURES

Mice, Beads Injection, and In Utero Lentiviral Injections

TβRII floxed mice (Levéen et al., 2002) were crossed to *K14-Cre* (Vasioukhin et al., 1999) and/or *Rosa26YFP$^{lox/stop/lox}$* (Srinivas et al., 2001) mice. Other mice were as published except for the *Bmpr1a$^{fl/fl}$;K15-CrePGR;Rosa26YFP$^{+/fl}$* cross. CD1 mice were from Charles River laboratories. Recombinant human TGF-β1, -β2, and -β3 (50–100 ng, R&D systems), mouse Noggin (200 ng, R&D systems), or BSA control was intradermally injected with FluoSpheres (Invitrogen). BrdU (50 μg/g) was injected intraperitoneally 12 and 24 hr before lethal administration of CO^2. Ultrasound-guided lentiviral injection and related procedures have been described (Beronja et al., 2010). Two controls were used as comparisons to knockdown mice: age- and sex-matched uninjected littermates and embryos infected with a nontargeting scrambled-shRNA, which activates the endogenous microRNA processing pathway but is not known to target any gene. All animals were maintained in an AAALAC-approved animal facility and procedures were performed with IACUC-approved protocols.

Statistical Analysis

Data were analyzed and statistics performed (unpaired two-tailed Student's t test) in Prism5 (GraphPad). Significant differences between two groups were noted by asterisks or actual p values.

Acknowledgments

References

Andl T, Ahn K, Kairo A, Chu EY, Wine-Lee L, Reddy ST, Croft NJ, Cebra-Thomas JA, Metzger D, Chambon P, et al. Epithelial Bmpr1a regulates differentiation and proliferation in postnatal hair follicles and is essential for tooth development. Development. 2004; 131:2257–2268. [PubMed: 15102710]

Beronja S, Livshits G, Williams S, Fuchs E. Rapid functional dissection of genetic networks via tissue-specific transduction and RNAi in mouse embryos. Nat Med. 2010; 16:821–827. [PubMed: 20526348]

Bierie B, Moses HL. Tumour microenvironment: TGFbeta: the molecular Jekyll and Hyde of cancer. Nat Rev Cancer. 2006; 6:506–520. [PubMed: 16794634]

Blanpain C, Fuchs E. Epidermal homeostasis: a balancing act of stem cells in the skin. Nat Rev Mol Cell Biol. 2009; 10:207–217. [PubMed: 19209183]

Blanpain C, Lowry WE, Geoghegan A, Polak L, Fuchs E. Self-renewal, multipotency, and the existence of two cell populations within an epithelial stem cell niche. Cell. 2004; 118:635–648. [PubMed: 15339667]

Botchkarev VA, Botchkareva NV, Nakamura M, Huber O, Funa K, Lauster R, Paus R, Gilchrest BA. Noggin is required for induction of the hair follicle growth phase in postnatal skin. FASEB J. 2001; 15:2205–2214. [PubMed: 11641247]

Chang C, Eggen BJ, Weinstein DC, Brivanlou AH. Regulation of nodal and BMP signaling by tomoregulin-1 (X7365) through novel mechanisms. Dev Biol. 2003; 255:1–11. [PubMed: 12618130]

Cheifetz S, Weatherbee JA, Tsang ML, Anderson JK, Mole JE, Lucas R, Massagué J. The transforming growth factor-β system, a complex pattern of cross-reactive ligands and receptors. Cell. 1987; 48:409–415. [PubMed: 2879635]

Cotsarelis G, Sun TT, Lavker RM. Label-retaining cells reside in the bulge area of pilosebaceous unit: implications for follicular stem cells, hair cycle, and skin carcinogenesis. Cell. 1990; 61:1329–1337. [PubMed: 2364430]

Enshell-Seijffers D, Lindon C, Kashiwagi M, Morgan BA. β-catenin activity in the dermal papilla regulates morphogenesis and regeneration of hair. Dev Cell. 2010; 18:633–642. [PubMed: 20412777]

Foitzik K, Paus R, Doetschman T, Dotto GP. The TGF-β2 isoform is both a required and sufficient inducer of murine hair follicle morphogenesis. Dev Biol. 1999; 212:278–289. [PubMed: 10433821]

Giacomini D, Páez-Pereda M, Stalla J, Stalla GK, Arzt E. Molecular interaction of BMP-4, TGF-β, and estrogens in lactotrophs: impact on the PRL promoter. Mol Endocrinol. 2009; 23:1102–1114. [PubMed: 19342445]

Greco V, Chen T, Rendl M, Schober M, Pasolli HA, Stokes N, Dela Cruz-Racelis J, Fuchs E. A two-step mechanism for stem cell activation during hair regeneration. Cell Stem Cell. 2009; 4:155–169. [PubMed: 19200804]

Guasch G, Schober M, Pasolli HA, Conn EB, Polak L, Fuchs E. Loss of TGFbeta signaling destabilizes homeostasis and promotes squamous cell carcinomas in stratified epithelia. Cancer Cell. 2007; 12:313–327. [PubMed: 17936557]

Haramis AP, Begthel H, van den Born M, van Es J, Jonkheer S, Offerhaus GJ, Clevers H. De novo crypt formation and juvenile polyposis on BMP inhibition in mouse intestine. Science. 2004; 303:1684–1686. [PubMed: 15017003]

Harms PW, Chang C. Tomoregulin-1 (TMEFF1) inhibits nodal signaling through direct binding to the nodal coreceptor Cripto. Genes Dev. 2003; 17:2624–2629. [PubMed: 14563676]

He XC, Zhang J, Tong WG, Tawfik O, Ross J, Scoville DH, Tian Q, Zeng X, He X, Wiedemann LM, et al. BMP signaling inhibits intestinal stem cell self-renewal through suppression of Wnt-β-catenin signaling. Nat Genet. 2004; 36:1117–1121. [PubMed: 15378062]

Horsley V, Aliprantis AO, Polak L, Glimcher LH, Fuchs E. NFATc1 balances quiescence and proliferation of skin stem cells. Cell. 2008; 132:299–310. [PubMed: 18243104]

Hsu YC, Pasolli HA, Fuchs E. Dynamics between stem cells, niche, and progeny in the hair follicle. Cell. 2011; 144:92–105. [PubMed: 21215372]

Izumi N, Mizuguchi S, Inagaki Y, Saika S, Kawada N, Nakajima Y, Inoue K, Suehiro S, Friedman SL, Ikeda K. BMP-7 opposes TGF-β1-mediated collagen induction in mouse pulmonary myofibroblasts through Id2. Am J Physiol Lung Cell Mol Physiol. 2006; 290:L120–L126. [PubMed: 16126788]

Jamora C, Lee P, Kocieniewski P, Azhar M, Hosokawa R, Chai Y, Fuchs E. A signaling pathway involving TGF-β2 and snail in hair follicle morphogenesis. PLoS Biol. 2005; 3:e11. [PubMed: 15630473]

Jian H, Shen X, Liu I, Semenov M, He X, Wang XF. Smad3-dependent nuclear translocation of β-catenin is required for TGF-β1-induced proliferation of bone marrow-derived adult human mesenchymal stem cells. Genes Dev. 2006; 20:666–674. [PubMed: 16543220]

Keller B, Yang T, Chen Y, Munivez E, Bertin T, Zabel B, Lee B. Interaction of TGFβ and BMP signaling pathways during chondrogenesis. PLoS ONE. 2011; 6:e16421. [PubMed: 21297990]

Kobielak K, Stokes N, de la Cruz J, Polak L, Fuchs E. Loss of a quiescent niche but not follicle stem cells in the absence of bone morphogenetic protein signaling. Proc Natl Acad Sci USA. 2007; 104:10063–10068. [PubMed: 17553962]

Koinuma D, Tsutsumi S, Kamimura N, Taniguchi H, Miyazawa K, Sunamura M, Imamura T, Miyazono K, Aburatani H. Chromatin immunoprecipitation on microarray analysis of Smad2/3 binding sites reveals roles of ETS1 and TFAP2A in transforming growth factor β signaling. Mol Cell Biol. 2009; 29:172–186. [PubMed: 18955504]

Kulessa H, Turk G, Hogan BL. Inhibition of Bmp signaling affects growth and differentiation in the anagen hair follicle. EMBO J. 2000; 19:6664–6674. [PubMed: 11118201]

Levéen P, Larsson J, Ehinger M, Cilio CM, Sundler M, Sjöstrand LJ, Holmdahl R, Karlsson S. Induced disruption of the transforming growth factor β type II receptor gene in mice causes a lethal inflammatory disorder that is transplantable. Blood. 2002; 100:560–568. [PubMed: 12091349]

Liu Z, Tang Y, Qiu T, Cao X, Clemens TL. A dishevelled-1/Smad1 interaction couples WNT and bone morphogenetic protein signaling pathways in uncommitted bone marrow stromal cells. J Biol Chem. 2006; 281:17156–17163. [PubMed: 16621789]

Massagué J. TGFbeta in cancer. Cell. 2008; 134:215–230. [PubMed: 18662538]

Massagué J, Andres J, Attisano L, Cheifetz S, López-Casillas F, Ohtsuki M, Wrana JL. TGF-β receptors. Mol Reprod Dev. 1992; 32:99–104. [PubMed: 1322148]

Millar SE. Molecular mechanisms regulating hair follicle development. J Invest Dermatol. 2002; 118:216–225. [PubMed: 11841536]

Moreno-Bueno G, Cubillo E, Sarrió D, Peinado H, Rodríguez-Pinilla SM, Villa S, Bolós V, Jordá M, Fabra A, Portillo F, et al. Genetic profiling of epithelial cells expressing E-cadherin repressors reveals a distinct role for Snail, Slug, and E47 factors in epithelial-mesenchymal transition. Cancer Res. 2006; 66:9543–9556. [PubMed: 17018611]

Nishimura EK, Suzuki M, Igras V, Du J, Lonning S, Miyachi Y, Roes J, Beermann F, Fisher DE. Key roles for transforming growth factor β in melanocyte stem cell maintenance. Cell Stem Cell. 2010; 6:130–140. [PubMed: 20144786]

Ovcharenko I, Nobrega MA, Loots GG, Stubbs L. ECR Browser: a tool for visualizing and accessing data from comparisons of multiple vertebrate genomes. Nucleic Acids Res. 2004; 32(Web Server issue):W280–W286. [PubMed: 15215395]

Plikus MV, Mayer JA, de la Cruz D, Baker RE, Maini PK, Maxson R, Chuong CM. Cyclic dermal BMP signalling regulates stem cell activation during hair regeneration. Nature. 2008; 451:340–344. [PubMed: 18202659]

Rabbani P, Takeo M, Chou W, Myung P, Bosenberg M, Chin L, Taketo MM, Ito M. Coordinated activation of Wnt in epithelial and melanocyte stem cells initiates pigmented hair regeneration. Cell. 2011; 145:941–955. [PubMed: 21663796]

Rendl M, Polak L, Fuchs E. BMP signaling in dermal papilla cells is required for their hair follicle-inductive properties. Genes Dev. 2008; 22:543–557. [PubMed: 18281466]

Rice RH, Green H. Presence in human epidermal cells of a soluble protein precursor of the cross-linked envelope: activation of the cross-linking by calcium ions. Cell. 1979; 18:681–694. [PubMed: 42494]

Schmidt-Ullrich R, Paus R. Molecular principles of hair follicle induction and morphogenesis. Bioessays. 2005; 27:247–261. [PubMed: 15714560]

Sekiya T, Oda T, Matsuura K, Akiyama T. Transcriptional regulation of the TGF-β pseudoreceptor BAMBI by TGF-β signaling. Biochem Biophys Res Commun. 2004; 320:680–684. [PubMed: 15240101]

Siegel PM, Massagué J. Cytostatic and apoptotic actions of TGF-β in homeostasis and cancer. Nat Rev Cancer. 2003; 3:807–821. [PubMed: 14557817]

Srinivas S, Watanabe T, Lin CS, William CM, Tanabe Y, Jessell TM, Costantini F. Cre reporter strains produced by targeted insertion of EYFP and ECFP into the ROSA26 locus. BMC Dev Biol. 2001; 1:4. [PubMed: 11299042]

Tanimura S, Tadokoro Y, Inomata K, Binh NT, Nishie W, Yamazaki S, Nakauchi H, Tanaka Y, McMillan JR, Sawamura D, et al. Hair follicle stem cells provide a functional niche for melanocyte stem cells. Cell Stem Cell. 2011; 8:177–187. [PubMed: 21295274]

ten Dijke P, Arthur HM. Extracellular control of TGFbeta signalling in vascular development and disease. Nat Rev Mol Cell Biol. 2007; 8:857–869. [PubMed: 17895899]

Vasioukhin V, Degenstein L, Wise B, Fuchs E. The magical touch: genome targeting in epidermal stem cells induced by tamoxifen application to mouse skin. Proc Natl Acad Sci USA. 1999; 96:8551–8556. [PubMed: 10411913]

Wang S, Hirschberg R. BMP7 antagonizes TGF-β-dependent fibrogenesis in mesangial cells. Am J Physiol Renal Physiol. 2003; 284:F1006–F1013. [PubMed: 12676736]

Wrighton KH, Lin X, Yu PB, Feng XH. Transforming growth factor β can stimulate Smad1 phosphorylation independently of bone morphogenic protein receptors. J Biol Chem. 2009; 284:9755–9763. [PubMed: 19224917]

Yew KH, Hembree M, Prasadan K, Preuett B, McFall C, Benjes C, Crowley A, Sharp S, Tulachan S, Mehta S, et al. Cross-talk between bone morphogenetic protein and transforming growth factor-β signaling is essential for exendin-4-induced insulin-positive differentiation of AR42J cells. J Biol Chem. 2005; 280:32209–32217. [PubMed: 16020542]

Zhang J, He XC, Tong WG, Johnson T, Wiedemann LM, Mishina Y, Feng JQ, Li L. Bone morphogenetic protein signaling inhibits hair follicle anagen induction by restricting epithelial stem/progenitor cell activation and expansion. Stem Cells. 2006; 24:2826–2839. [PubMed: 16960130]
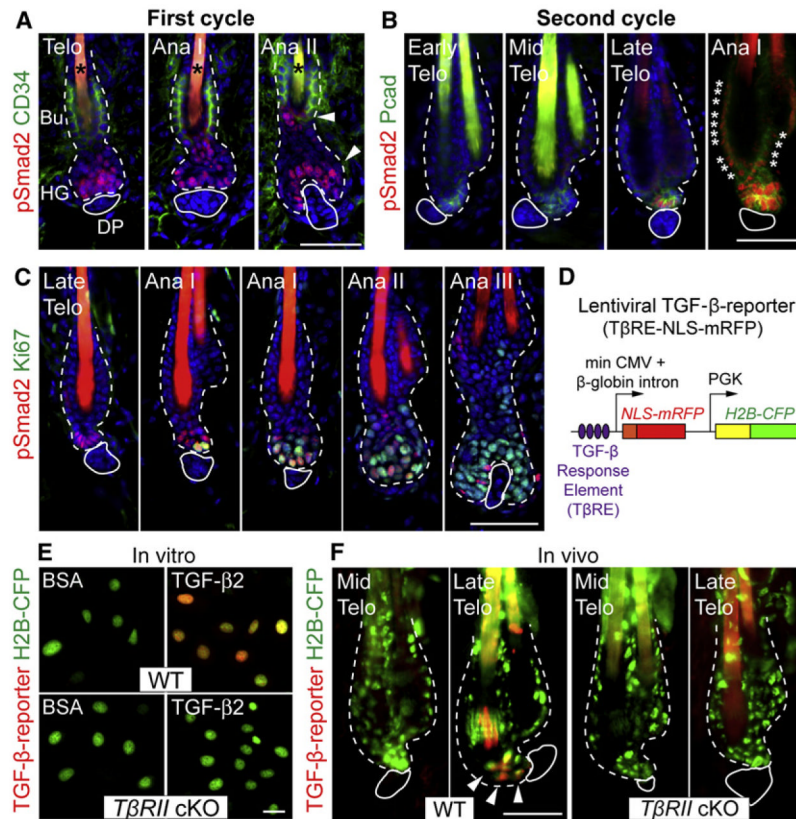
Figure 1. TGF-β Signaling Is Transiently Activated in HFSCs at the Telogen→Anagen Transition of the New Hair Cycle

(A) pSmad2 and CD34 immunolocalizations in HFs during the first telogen→anagen transition; telogen (postnatal day 21, P21), anagen I (P22), and anagen II (P23). Note two distinct sites of pSmad2 staining (arrowheads). Black asterisks denote autofluorescence (not immunostaining) on the hair shaft.

(B) Time-course monitoring of pSmad2 and P-cadherin (Pcad) during the extended second telogen and into the next anagen. White asterisks denote low but real pSmad2 in bulge HFSCs.

(C) pSmad2 and Ki67 coemerge upon HFSC activation. TGF-β signaling is transient and wanes after the telogen→ anagen transition.

(D) Lentiviral TGF-β-reporter. H2B-CFP driven by a constitutively active *PGK* promoter is used as a viral infection marker; NLS-mRFP reports TGF-β-pSmad2 signaling.

(E) Validation of the TGF-β-reporter in 1°MK cultured from WT and *TβRII*-cKO skins. Note that reporter activity occurs only if TβRII is intact and cells are stimulated with TGF-β2.

(F) Verification that canonical TGF-β signaling (NLS-mRFP[+]; arrowheads) occurs in HG SCs during late (P74) telogen. The TGF-β-reporter was transduced specifically into the surface epithelium by in utero infection of live E9.5 embryos.

Dashed lines denote dermal-epidermal border; solid lines delineate the DP. Blue channel is DAPI staining. Scale bars represent 50 μm. See also Figure S1.
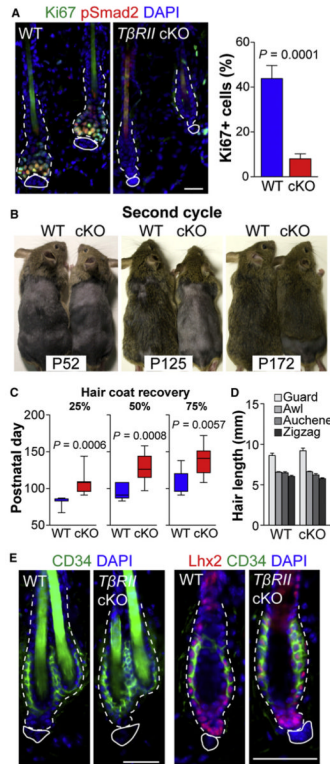
Figure 2. Mice whose Skin Epithelium Is Deficient in TGF-β Signaling Show a Delay in HFSC Activation and Hair Cycle Entry

(A) Immunolocalization of Ki67 and pSmad2 in WT and *TβRII*-cKO mice (P22). Dashed and solid lines outline HFSC bulge/HG niche and DP, respectively. Quantification of Ki67$^+$HG cells (n=5, 96 HG cells in each mice) shown at right. (B and C) Hair coats of pairs of WT and *TβRII*-cKO mice were clipped in mid-second telogen (P52) and then photographed periodically thereafter and categorized according to 25%, 50%, or 75% recovery. WT, n = 9; *TβRII*-cKO, n = 8 (n stands for mouse number). Note that hair coat recovery in WT mice was nearly complete by P125, but in *TβRII*-cKO-matched littermates, recovery still often lagged even at P172. Box-and-whisker plots: mid-line, median; box, 25th and 75th percentiles; whiskers, minimum and maximum.

(D) Analysis of the four types of hairs plucked at telogen (Guard, n = 10; Awl, n 21; Auchene, n 16; and Zigzag, n 20).

(E) Immunolocalizations of bulge-specific CD34 and bulge/HG marker Lhx2 in telogen-phase HFs. Data are mean ± SEM.
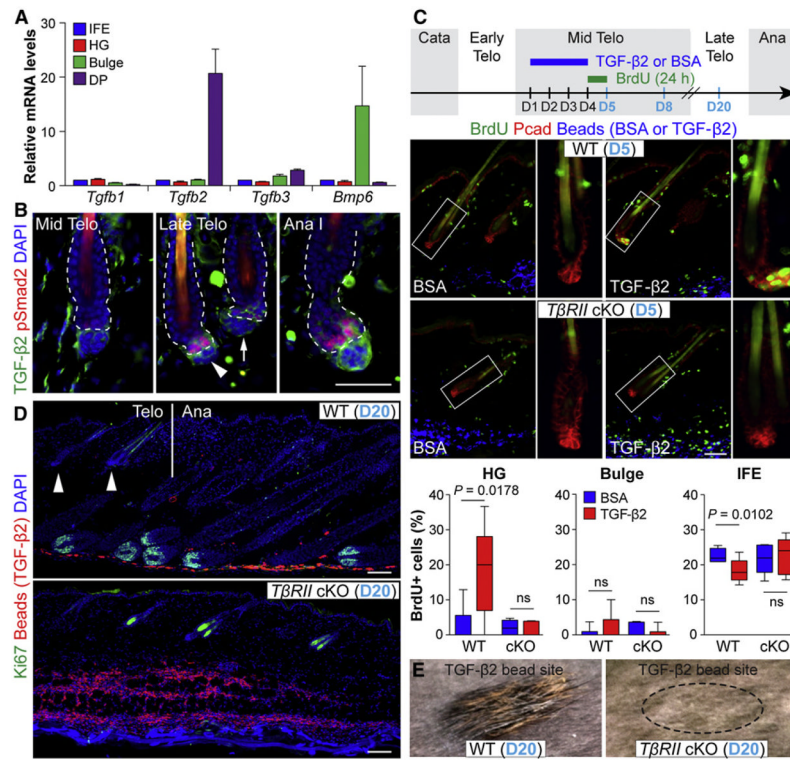
Scale bars represent 50 μm.

Figure 3. TGF-β2 Is Produced by DP, Activates pSmad2 in HFSCs, and Participates in the Telogen→Anagen Transition

(A) RT-qPCR on mRNAs from IFE, HG, bulge, and DP cells FACS purified from *Lef1-RFP* and *TβRII-Het/Rosa26YFP* HFs in late telogen (P70).

(B) Immunolocalization of TGF-β2 and pSmad2 at the DP-HG interface is low through mid-telogen (P56) but elevates in late (P65) telogen through early anagen (Ana I, P72). Note: late-telogen HF with strongest TGF-β2 in DP shows highest pSmad2 in HG (arrowhead versus arrow). Dashed lines denote dermal-epidermal border.

(C–E) Precocious activation of telogen→anagen occurs when TGF-β2-soaked fluorescent beads are injected intradermally.

(C) (Top) Experimental strategy. TGF-β2 or BSA was coinjected with blue or red fluorescent beads intradermally at days 1–3, followed by BrdU administration at D4 and analysis at days 5, 8, or 20. (Middle) TGF-β2 accelerates BrdU immunodetection in WT, but not *TβRII*-cKO HG. (Right) Magnified views of boxed areas. (Bottom) Quantifications of BrdU incorporation into HG (Pcad+), bulge (CD34+), and IFE (K5+ other) cells from mice injected with either BSA (n = 6) or TGF-β2 (n   6). Box-and-whisker plots: mid-line, median; box, 25th and 75th percentiles; whiskers, minimum and maximum.

(D) Ki67 immunolabeling of skin sections from (E). Vertical line denotes boundary between telogen and anagen WT HFs, correlating with bead (TGF-β2) density in the vicinity.

(E) Surface views of TGF-β2-injected areas at D20. Precocious hair growth was observed only on WT skin. Dashed circle indicates still barren injection site on *TβRII*-cKO animal. Data are mean ± SEM.

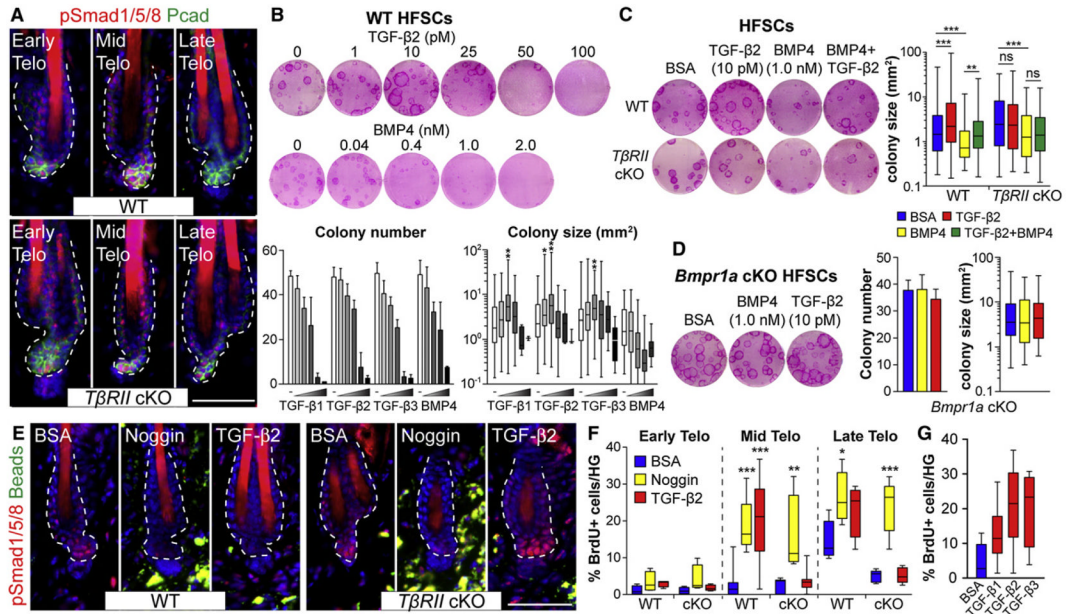Scale bars represent 50 μm. See also Figure S2.

Figure 4. TGF-β Stimulates Colony Formation of Primary HFSCs In Vitro and Dampens BMP Signaling in HFSCs In Vivo

(A) Immunolocalizations of pSmad1/5/8 in early (P48), mid (P59), and late (P72) second-telogen WT (*TβRII*-Het) and *TβRII*-cKO HFs. Note that nuclear pSmad1/5/8 (BMP signaling) wanes in late-telogen WT but not *TβRII*-cKO HFs.

(B) Bulge SCs were FACS purified from telogen-phase HFs, plated, and allowed to grow for 2 weeks in media supplemented with TGF-β2 or BMP4 at concentrations indicated. Quantifications of colony numbers and sizes are shown below.

(C and D) Colony formation assays on HFSCs from (C) WT and *TβRII*-cKO or (D) *Bmpr1a*-cKO HFs exposed to TGF-β2 (10 pM) and/or BMP4 (1.0 nM) for 2 weeks. Quantifications of (C, D) colony sizes and (D) numbers are shown right.

(E) BSA, Noggin, or TGF-β2 was coinjected with green fluorescent beads intradermally into *TβRII*-Het/WT and cKO mice in mid-telogen (P58–P60), and then examined for BMP signaling (anti-pSmad1/5/8) in HFSCs.

(F) Quantifications of BrdU incorporated into HG cells near the sites of bead injections. BrdU was administered intraperitoneally for 24 hr after the intradermal injections of BSA, Noggin, or TGF-β2 at early (P48–P50, n = 4) and mid (P58–P60, n = 4–13) telogen and the telogen→anagen transition (P73–P75, n = 5).

(G) Quantifications of BrdU incorporated into HG cells near the injection sites (n ≥ 6). Blue channel is DAPI. Dashed lines denote dermal-epidermal border. Data are mean ± SEM. Box-and-whisker plots: mid-line, median; box, 25th and 75th percentiles; whiskers, minimum and maximum. ***p < 0.001, **p < 0.01, *p < 0.05. Scale bars represent 50 μm. See also Figure S3.
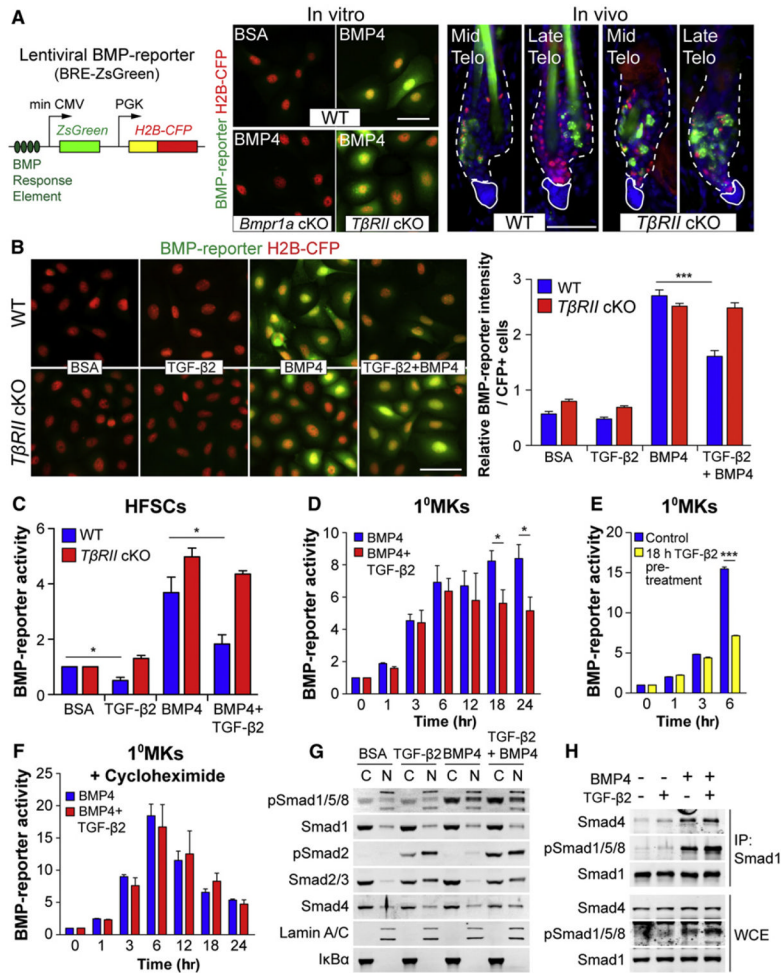
Figure 5. Evidence Favoring a TGF-β Target Gene Mechanism for Dampening BMP Signaling rather than pSmad2/3-Mediated Competition for Limiting Smad4

(A) Lentiviral BMP-reporter. (In vitro) After BMP4 stimulation, BMP-reporter activity (green) is detected in 1°MK from WT and *TβRII*-cKO, but not *Bmpr1a*-cKO (*Bmpr1a^fl/fl*;*K14-Cre*) mice. (In vivo) BMP-reporter activity in HFs at mid (P58) and late (P74) telogen. Note that BMP-reporter activity fails to be downregulated in *TβRII*-cKO HFs. Dashed lines, dermal-epidermal border; solid lines, DP; DAPI (blue).

(B–F) Lentiviral BMP-reporter-transduced 1°MKs (B, D–F) or 1°HFSCs from FACS-purified HGs (C) were plated and stimulated with BSA, TGF-β2, and/or BMP4 for 24 hr.

(B) Fixed cells were observed by direct-fluorescence microscopy. (Right) Quantifications of ZsGreen fluorescence intensity in H2B-CFP+ cells (n = 10,   370 H2BCFP + cells were measured at the same exposure time).

(C–F) RT-qPCR analyses of *ZsGreen* mRNA levels. Lentiviral BMP-reporter-transduced cells were stimulated with BMP4 ± TGF-β2 for either 24 hr (C) or indicated times (D–F), and BMP-reporter activities were quantified by *ZsGreen* mRNA levels.

(E) Cells ± TGF-β2 pretreatment for 18 hr were stimulated with BMP4 for indicated times.

(F) Cells were plated in the presence of BMP4 ± TGF-β2, and cycloheximide (10 or 100 μM) was then added for indicated times. Data shown are for 10 μM cycloheximide, but similar results were obtained with 100 μM.

(G) Immunoblot analyses of nuclear (N) and cytoplasmic (C) fractions from 1°MK treated with TGF-β2 and/or BMP4. Nuclear control: anti-Lamin A/C; cytoplasmic control: anti-IκBα.

(H) Coimmunoprecipitation of endogenous Smad4 and Smad1 in TGF-β2 and/or BMP4-treated 1°MK. Complexes (IP) and whole cell extracts (WCE) were analyzed by immunoblotting with the indicated antibodies.

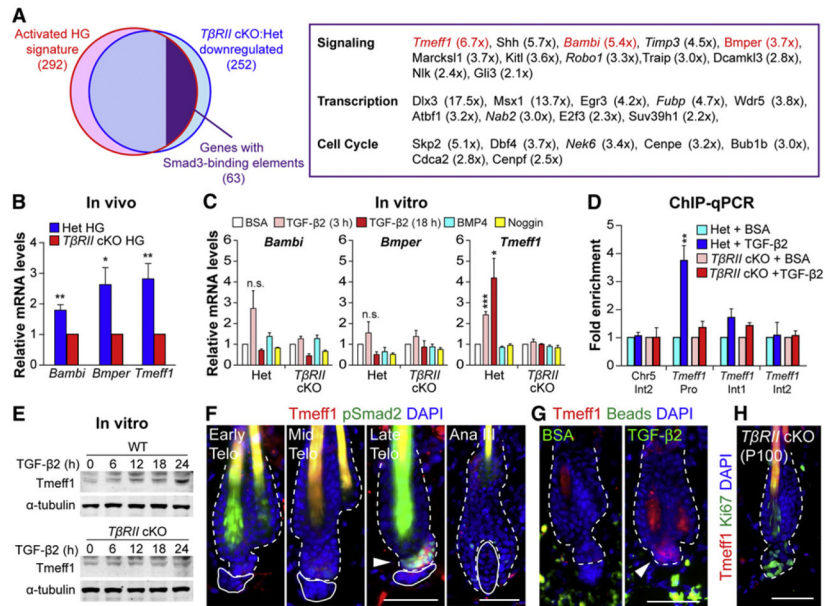Data are mean ± SEM. ***$p < 0.001$, *$p < 0.05$. Scale bars represent 50 μm.

Figure 6. *Tmeff1* Is a Direct Target Gene of TGF-β Signaling and Expresses in the Hair Germ at the Telogen→Anagen Transition

(A) Schematic summary of microarray analysis. Overlap between the activated HG signature and the list of genes downregulated by ≥ 2× in late-telogen/early-anagen *TβRII*-cKO versus Het HGs. 63 of these genes (see representative examples at right) contain putative conserved Smad2/3 binding elements. Italicized genes are among the 1,787 genes bound by Smad2/3 in TGF-β-stimulated HaCaT keratinocytes (Koinuma et al., 2009).

(B) RT-qPCR on independently derived in vivo mRNA samples.

(C) RT-qPCR on in vitro mRNAs from *TβRII*-Het and null 1°MK stimulated with BSA, TGF-β2 (3 and 18 hr), BMP4 (3 hr), or Noggin (3 hr). Data are means ± SEM of three independent experiments.

(D) *Tmeff1* ChIP analyses with a Smad2/3 antibody in BSA- or TGF-β2-treated *TβRII*-Het and null 1°MK. Each primer set was designed to encompass three conserved Smad-binding motifs at the *Tmeff1* locus as predicted by ECR Browser (Ovcharenko et al., 2004). Fold-enrichments of immunoprecipitated DNA fragments are compared to a control intronic fragment with no predicted site (Chr5-Int2). Data are shown as means ± SEM of two independent experiments.

(E) Immunoblotting of lysates prepared from WT and *TβRII*-null 1°MK stimulated with TGF-β2 for indicated times.

(F) Coimmunolocalization of Tmeff1 and pSmad2 specifically at late telogen (P74, arrowhead) and not early (P46) or mid (P58) telogen or early anagen (P80).

(G) Tmeff1 immunodetection (arrowhead) in skin sections of sites where BSA or TGF-β2 was coinjected with green fluorescent beads in mid-telogen skin.

(H) Immunodetection of Tmeff1 and Ki67 in the nearly 20 days delayed early anagen *TβRII*-cKO HF. Note that Tmeff1 expression is absent even though the HG has initiated proliferation.

Dashed lines denote dermal-epidermal border; solid lines delineate the DP. Data are mean ± SEM. ***p < 0.001, **p < 0.01, *p < 0.05. Scale bars represent 50 μm. See also Figure S4.
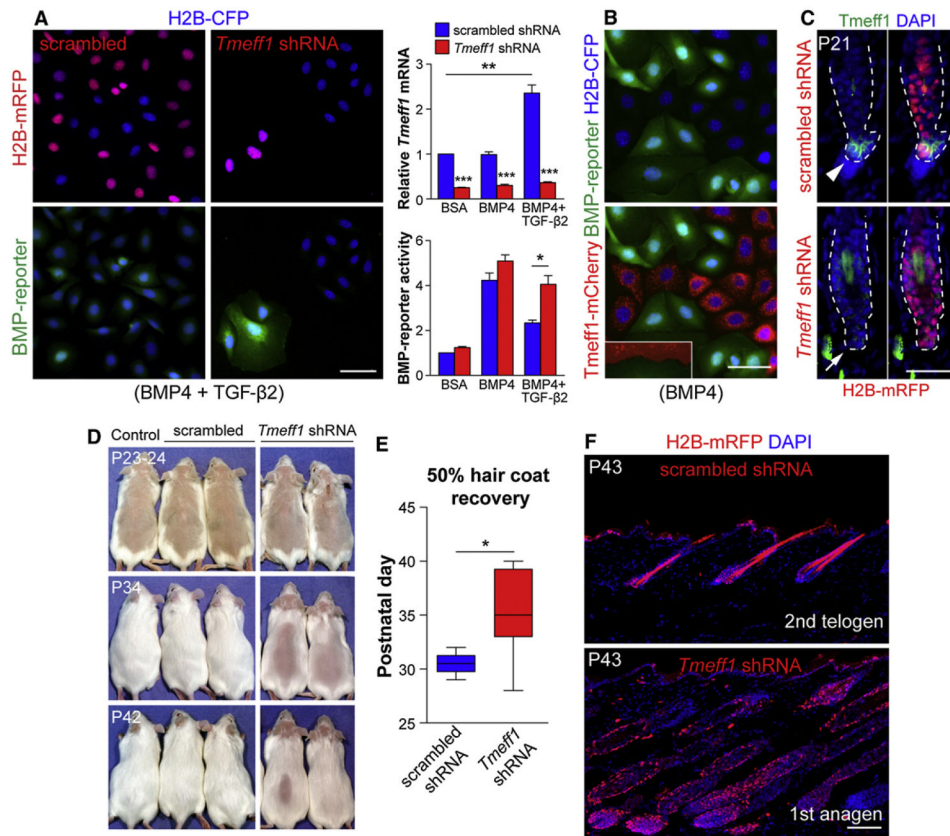
Figure 7. Tmeff1 Mediates the Dampening Effect of TGF-β2 on BMP Signaling

(A) 1°MK transduced for the BMP-reporter (H2B-CFP is transduction marker) were also transduced with lentivirus harboring either scrambled control or *Tmeff1*- shRNAs (H2B-mRFP is transduction marker). Cells were then treated with BMP4 ± TGF-β2 for 24 hr. (Right) RT-qPCR of indicated mRNAs. FACS was used to enrich for shRNA-infected BMP-reporter cells, which were then stimulated with BMP4 ± TGF-β2 for 24 hr.

(B) The BMP-reporter 1°MK (H2B-CFP is transduction marker) were transfected with an expression vector encoding Tmeff1-mCherry and stimulated with BMP4 for 24 hr. Inset shows that some of the overexpressed Tmeff1-mCherry protein is at the membrane, consistent with the corresponding functional readout of reduced BMP-reporter expression.

(C–F) Embryos were infected with *Tmeff1*-shRNA or scrambled control shRNA lentiviruses (H2B-mRFP[+]) at E9.5 and then analyzed as adult mice.

(C) Representative anti-Tmeff1 immunofluorescence sections of P21 skins. Merged green and red channels are at right. Dashed lines denote dermal-epidermal border.

(D) Hair coats were shaved at the start of the first postnatal anagen and regrowth was monitored thereafter at times indicated. Note: scrambled and uninfected (control) littermates were indistinguishable. Representative examples are shown, but some experimental variation was observed, presumably because of variations in infection efficiency and/or relative timing of infection.

(E) Quantification of 50% hair coat recovery from data in (D). Scramble control, n = 6; *Tmeff1*-shRNA, n = 10 (n stands for mouse number).

Box-and-whisker plots: mid-line, median; box, 25th and 75th percentiles; whiskers, minimum and maximum.

(F) At P43, HFs transduced with the scrambled control had already entered the second telogen, while similar transductions but with a *Tmeff1*-shRNA virus resulted in HFs that were still delayed in anagen of the first postnatal hair cycle.

Data are mean ± SEM. ***p < 0.001, **p < 0.01, *p < 0.05. Scale bars represent 50 µm. See also Figure S5.